ANALYSIS OF SILOXANE MIXTURES USED IN ORGANIC RANKINE CYCLE WITH THERMAL STABILITY LIMITS

Wenhuan Wang [1], Xiaoye Dai [1*], Lin Shi [1]

[1]Tsinghua University, Department of Energy and Power Engieering, Beijing, China

*Corresponding Author: daixy@mail.tsinghua.edu.cn

ABSTRACT

The siloxanes and their mixtures are suitable working fluids for organic Rankine cycle (ORC) systems with high-temperature heat sources. The thermal stability of siloxanes has a significant effect on the working fluid selection and cycle performance of ORCs. In this study, a thermal decomposition experimental system is designed to measure the thermal stability of octamethyltrisiloxane (MDM), and the effects of the hexamethyldisiloxane (MM) mass fraction and evaporation temperature on the net power and thermal efficiency are calculated. The results showed that the decomposition of MDM could be detected at 240℃ and had higher decomposition ratios comparing with MM. With the temperature limit, the net power and thermal efficiency are both lower than those without the evaporation temperature limit. Siloxane mixtures are the better choice for ORC systems using siloxanes as working fluids in conditions of this paper. MM/MDM (0.6/0.4) improves the net power and heat efficiency of the system by 8.1% and 1.7% respectively, comparing with that of the pure working fluids.

1 INTRODUCTION

Industrial waste heat recovery and renewable energy utilization have attracted more attention to solve energy and environmental problems. The organic Rankine cycle (ORC) has been widely used in solar power (Tchanche *et al*, 2011), geothermal power (Yildirim and Ozgener, 2012), biomass power (Strzalka *et al*, 2017), and industrial waste heat recovery systems (Velez et al, 2012) because of their high thermal efficiencies and easy realization (Kim et al, 2017), (Shu et al, 2017). The ORCs are suitable for a wide range of operating temperatures. The medium- and low-temperature geothermal energy has become a main heat source for installed ORC systems in the world (Tartière and Astolfi, 2017). The ORC systems with high-temperature heat sources have recently attracted much intetest due to their higher thermal efficiency (Zhang *et al*, 2021). For high-temperature organic Rankine cycle, the selection of the working fluids is very important. Siloxanes are considered suitable working fluids because of their low toxicity, non-flammability, high critical temperatures, and especially good thermal stability at high temperatures (Angelino and Paliano, 1998), (Erhart *et al*, 2016), (Dai *et al*, 2019), (Preißinger and Brüggemann, 2016).

Some studies showed that mixture working fluids could improve the performance of the ORC system. Zhou *et al*. (2016) analyzed an organic Rankine cycle system with the zeotropic mixture R245fa/R227ea as working fluid using the thermodynamic first law and the second law. The results showed that the optimized ORC with R245fa/R227ea could generate 24.7% more power than that with R227ea as working fluid. Tian *et al*. (2017) selected three zeotropic mixtures consisting of R123 and various concentrations of siloxanes as the working fluid in an ORC system. The results showed that the system with D_4/R123 (0.3/0.7) presented the best thermodynamic performance with the largest net power of 21.66 kW and the highest thermal efficiency of 22.84%. Dong *et al*. (2014) investigated the performance of high-temperature ORC with siloxane mixtures as working fluid. The mixture MM/MDM with a ratio of 0.4/0.6 was considered to be the optimal working fluid with a maximum first law efficiency of 16.88%, representing a relative increase of 9.40% for MM and 5.96% for MDM, respectively. Oyekale

et al. (2020) proposed that mixture MM/MDM with a ratio of 0.9/0.1 and 0.8/0.2 could increase the net power by 2% and 1.4% respectively. However, all organics including siloxanes will decompose at high temperatures, which can lead to serious problems for ORC systems. For example, the solid decomposition products may block the tubes or add the thermal resistance of the heat exchange surface. More seriously, some possible corrosive products can destroy system materials and lead to safety problems. Thus, further studies on the performance of ORCs with siloxane thermal stability limits are required.

There have been some experimental results about the thermal stability of MM and MDM in previous studies. Dai *et al*. (2019) and Preißinger and Brüggemann (2016) measured the decomposition ratios of MM at different temperatures. Keulen *et al*. (2018) measured the vapor pressure differences of MM and MDM at different temperatures and appreciable decomposition temperatures were detected as 240°C and 260°C respectively. In this work, the decomposition ratios of MDM at different temperatures were measured in comparison with those of MM (Section 2). A thermal decomposition experimental system was designed and the thermal stability of MDM was measured using it.

Rajabloo *et al*. (2017) analyzed the effects of thermal decomposition on ORC system using an off-design model. The results showed that the fluid decomposition has big effects on cycle performance, especially when the decomposed products are volatile. In this work, the cycle performance with thermal stability temperature limits was calculated in comparison with the theoretical performance without thermal stability temperature limits (Section 3). The performance of the ORC system with mixtures of MM and MDM as working fluids was analysed in this work.

2 EXPERIMENTS

2.1 Experimental system and method

MM and MDM are the main siloxane working fluids in the ORC system. In this work, MDM was selected as test fluid. The experimental results were compared with the thermal decomposition experimental results of MM. The samples of MDM and MM were obtained from commercial suppliers with purities higher than 97% and 99% respectively. The fluid properties are listed in Table 1.

Table 1: Fluid properties of test siloxanes.

Siloxane	molecular formula	T_b/°C	T_c/°C	P_c/MPa
MM	$C_6H_{18}Si_2$	100.25	245.60	1.94
MDM	$C_8H_{24}O_2Si_3$	152.51	290.94	1.42

The test system is shown in Fig. 1. The high-temperature reactor was made of 316L stainless steel with an internal volume of 25 mL, which had good corrosion resistance at high temperatures. The reactor was sealed by graphite washers and bolts. The maximum pressure of the reactor was 20 MPa and the maximum temperature was 400°C. Four reactors were installed in a heating furnace to reduce the experimental errors. The control valves were used to fill and discharge working fluids, and a safety valve was used to prevent damages caused by excessive pressure. A thermocouple and PID controller were used to control the temperature of the heating furnace and keep the temperature at a stable value. Before each experiment, the air in the reactor was evacuated using a vacuum pump to avoid the effects of air on the decomposition.

The experimental temperatures were set to be 240°C, 260°C, 280°C, 300°C, 320°C respectively, and then a reasonable pressure was set to ensure that the working fluid is in a gaseous state when heated in the reactor. The working fluid density in experimental conditions was calculated by the commercial software REFPROP 10.0. Then, the filling mass was equal to the density times the reactor volume. The filling procedure was at room temperature using a syringe and the injection mass uncertainty was ±0.05 g. All valves were closed after the filling procedure. The reactors were then placed in the heating furnace

and were heated to the set temperature. The experimental period was 24 h for each experiment. After the heating, the gaseous decomposition products of MDM were collected by gas bags and the mass of them was confirmed by measuring the mass of residual liquid sample. The gaseous and liquid decomposition products of MDM were analyzed by gas chromatography (GC) and GC-mass spectrometry (MS). More than four repeated experiments were conducted for each experimental condition and the averages of repeated experiments were considered as final results to reduce random errors. The standard deviation of the repeated experiment data was considered as the experimental uncertainty approximately. The decomposition ratio was defined as Equation 1:

$$r_A = \frac{x_{A,0} - x_{A,d}}{x_{A,0}} \times 100\% \quad (1)$$

where r_A is the decomposition ratio of fluid A, $x_{A,0}$ is the mass fraction of fluid A in the original sample, and $x_{A,d}$ is the mass fraction of fluid A in the sample after decomposition.

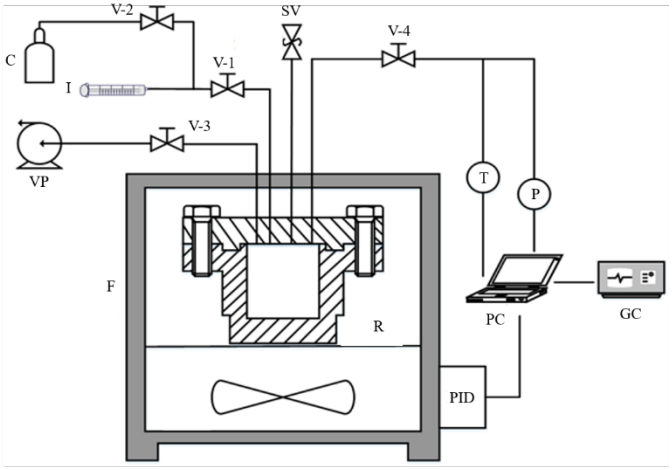

R: Reactor F: Heating Furnace V: Control Valve C: Gas cylinders
I: Liquid Injector P: Pressure sensor SV: Safety valve VP: Vacuum pump
PID: Temperature controller GC: Gas Chromatography T: Thermocouple
PC: Computer for data collection and system control

Figure 1: Schematic of the test system

2.2 Experimental results and discussion

The decomposition ratios of MDM with different temperatures are shown in Fig. 2. The results showed that the effect of temperatures on MDM thermal decomposition was significant. The decomposition ratio of MDM increased with the increasing heating temperature. The thermal decomposition had occurred at 240°C with MDM decomposition ratio of 2.95%. The decomposition ratio increased continuously with increasing temperatures and was 6.64% at 320°C.The decomposition ratios of MM with different temperatures (Dai *et al*, 2019) are also shown in Fig. 2 as the comparison. The results of MM were obtained using the same experimental system and method in this paper, so the results could be compared with those of MDM directly. The results showed that the decomposition ratios of MDM were obviously higher than those of MM in the temperature range of 240~320°C. The species and mass fractions of products (320℃, 24 h) in one of the MDM samples after decomposition are listed in Table 3. The results showed that MM was the main product of MDM thermal decomposition with the much smaller mass fractions of other products.

The experimental results showed that the decomposition of MM and MDM could be detected at 240°C. Thus, 220℃ was assumed to be the maximum evaporation temperature for ORC systems using the mixtures of MM and MDM as working fluids in the next section. It may be not the precise safe temperature for siloxanes, but can be convenient for the analysis in Section 3.

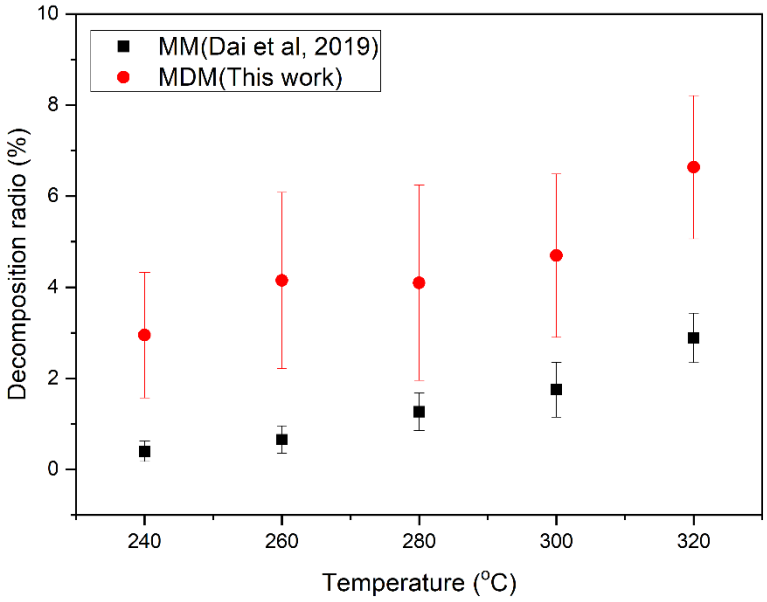

Figure 2: Decomposition ratios of MM (Dai *et al*, 2019) and MDM with different temperatures

Table 2: Product detection results at 320°C

Product	Mass fraction/%	Products	Mass fraction/%
MDM	90.47	MM	5.82
MD_2M	1.85	MD_3M	0.57
MD_4M	0.28	MD_5M	0.20
D_4	0.35	D_5	0.14
QM_4	0.23	Others	0.09

3 SYSTEM SIMULATION

3.1 System Description

The schematic of the ORC system and the temperature–entropy curve of the cycle using 0.6/0.4 MM/MDM as working fluid are shown in Fig. 3(a) and Fig. 3(b), respectively. The temperature profiles of mixtures matched with the heat source and sink better due to the temperature slides of mixtures. The cycle thermodynamic parameters of the ORC system are listed in Table 3. Hot air was selected as the heat source of the cycle. The inlet temperature of the heat source was 300°C, and the mass flow rate was 1 kg/s. The cooling water was selected as the cold source with an inlet temperature of 25°C. The evaporator pinch and condenser pinch were 10°C and 5°C, respectively. The isentropic efficiencies of the pump and expander were 0.9 and 0.85, respectively.

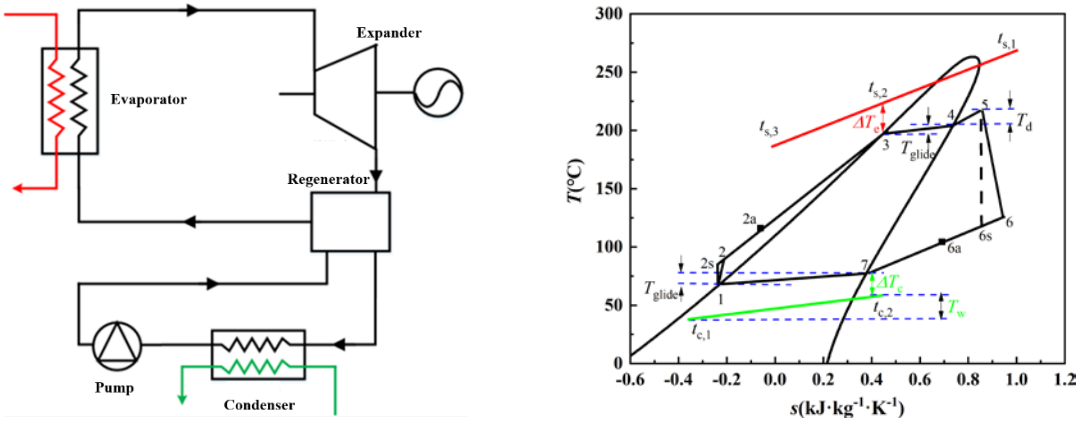

(a) (b)

Figure 3: Schematic of the ORC system (a) and saturated T–s curve of the ORC (b)

Table 3 Cycle thermodynamic design parameters

Parameters	Unit	Value
Heat source (air) temperature	$t_{s,1}$/°C	300
Heat source flow	$\dot{m}_s$/kg·s^{-1}	1
Cold source (water) temperature	$t_{c,1}$/°C	25
Evaporator pinch	ΔT_e/°C	10
Condenser pinch	ΔT_c/°C	5
Expander design isentropic efficiency	η_t/ %	85
Pump design isentropic efficiency	η / %	90

3.2 Assumption and Model Equation

The simulation model of the ORC system was designed using MATLAB with the fluid property database from REFPROP Version 10.0. Several assumptions were defined before modeling:
(1) The components in the cycle operate at a steady state.
(2) The heat exchangers in the cycle are counter-flow.
(3) The heat loss and fluid pressure drop in the pipeline are ignored.

For the evaporator, different pinch points can confirm different mass flows of working fluids. If the evaporator pinch appears in the position shown in Fig. 3, the mass flow of the working fluid can be calculated using the following equation:

$$\dot{m}_s\left(h_{s,1}-h_{s,2}\right)=\dot{m}_{wf}\left(h_5-h_3\right) \tag{2}$$

where the $\dot{m}_s$ and $\dot{m}_0$ represents the mass flow of heat source and working fluid, respectively. If The pinch point appears at the inlet of the evaporator, the mass flow of the working fluid can be calculated using the following equation:

$$\dot{m}_s\left(h_{s,1}-h_{s,3}\right)=\dot{m}_{wf}\left(h_5-h_{2a}\right) \tag{3}$$

$$h_{2a}=\alpha h_6+(1-\alpha)h_2 \tag{4}$$

where h_{2a} represents the enthalpy value of the working fluid at the outlet of the regenerator. The regenerative steam extraction rate α was set as 0.2. The heat transfer rate, net power, and thermal

efficiency can be calculated as:

$$Q_e = \dot{m}_{wf}\left(h_5 - h_{2a}\right) \tag{5}$$

$$Q_c = \dot{m}_{wf}\left(h_{6a} - h_1\right) \tag{6}$$

$$W_{net} = W_t - W_p \tag{7}$$

$$\eta_{th} = \frac{W_t - W_p}{Q_e} \tag{8}$$

where W_t and W_p represent power output of the expander and power consumption of the pump respectively, and can be calculated using the following equations:

$$W_t = \dot{m}_o\left(h_5 - h_{6s}\right)\eta_t = \dot{m}_o\left(h_5 - h_6\right) \tag{9}$$

$$W_p = \frac{\dot{m}_{wf}\left(h_{2s} - h_1\right)}{\eta} = \dot{m}_{wf}\left(h_2 - h_1\right) \tag{10}$$

3.3 Simulation results and Discussion

The thermal efficiency and net power of the system with different mixing ratios were calculated to compare the thermal performance of mixture and pure working fluid. Firstly, the maximum net power and the corresponding thermal efficiency of the subcritical system were analyzed without limiting the evaporation temperature. Then, the maximum evaporation temperature was limited to 220℃. The same calculation was performed, and the maximum net power and corresponding thermal efficiency of the system under a specific evaporation temperature range were obtained.

The calculation results are shown in Fig. 4. The results showed that the net power and thermal efficiency of some mixtures were all higher than that of the pure working fluid. The results also presented that the net power and thermal efficiency both decreased when the evaporation temperature was limited to 220℃. The decrease of thermal efficiency was significant while the decrease of net power was limited.

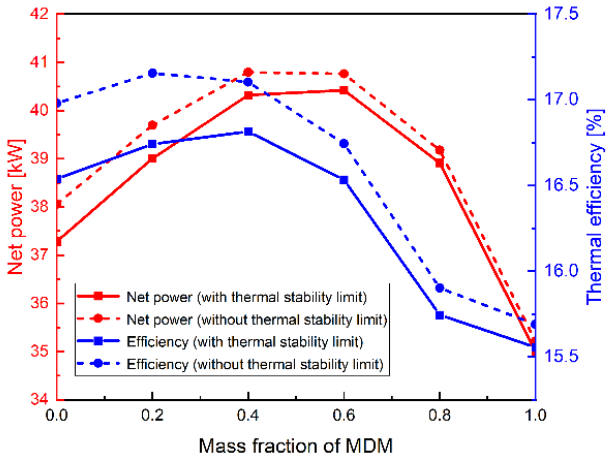

Figure 4: The net power and thermal efficiency changes with different mass fractions of MDM

The net power and thermal efficiency changes with different evaporation temperatures are shown in Fig. 5(a) and Fig. 5(b), respectively. The results showed that the net power of the system first increased slightly and then decreased sharply with the increasing evaporation temperature for all working fluids with different mixing ratios. The sharp decrease was caused by the changed pinch position of the evaporator, which led to small evaporator heat transfer rate from the heat source. The maximum net

power of mixtures appeared in the evaporation temperature range of 220°C to 250°C, which all exceeded the limit of evaporating temperature. However, the maximumn net power of mixtures with limited evaporation temperatures only decreased by 0.6%-2.0% comparing with theoretical maximumn values without evaporation temperature limits. Thus, the effect of the thermal stability limit on the net power was limited.

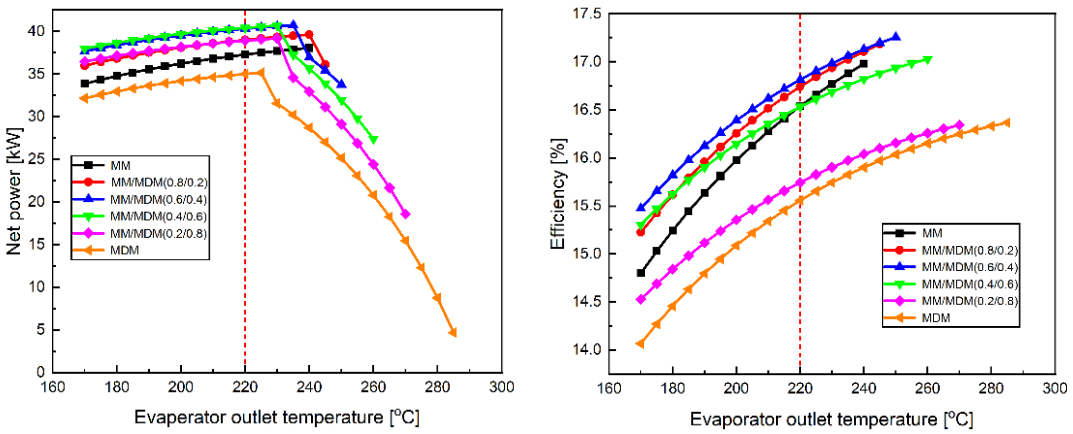

(a) (b)

Figure 5: The net power and thermal efficiency changes with different evaporation temperatures

The thermal efficiency of the system increased significantly with the increasing evaporation temperature. The results showed that the thermal efficiency of the system decreased significantly when the evaporation temperature was limited to 220°C. Thus, the higher evaporation temperature should be selected to improve the thermal efficiency of the system if the thermal efficiency is considered as the primary evaluation factor. If the net power is considered as the primary evaluation factor of ORC system design, the evaporation temperature should be limited to 220°C or even a lower temperature with an acceptable net power loss to ensure the safety and stability of the system.
These results also indicated that the MM/MDM (0.6/0.4) improved the net power and heat efficiency of the system by 8.1% and 1.7% respectively, which could be considered as better working fluid of these ORCs.

4 CONCLUSIONS

In this study, a thermal decomposition experimental system was designed and the thermal stability of MDM was measured using it. The effects of the MM mass fraction and evaporation temperature on the net power and thermal efficiency were calculated. The conclusions are summarized as follows:

- The obvious thermal decomposition of MDM has occurred at 240°C and the decomposition ratios of MDM were higher than those of MM in the temperature range of 240~320°C. The main decomposition products of MDM were liquid products like kinds of siloxanes, and MM had the biggest mass fraction in the MDM decomposition products.

- The net power and thermal efficiency of the system with the evaporation temperature limit were both lower than those without the evaporation temperature limit. The effect of the temperature limit on the net power was limited, while the decrease of thermal efficiency was more obvious.

- Some siloxane mixtures have better performance than the pure fluid with the system model and conditions in this paper and MM/MDM (0.6/0.4) can be considered as the optimal working fluid selection in this work.

NOMENCLATURE

h	specific enthalpy	(kJ/kg)
m	mass flow	(kg/s)
Q	heat flow rate	(kW)
r	decomposition ratio	(–)
W	power output	(kW)
x	mass fraction	(–)
η	efficiency	(–)
α	regenerative ratio	(–)

Subscript

1–7	state point
c	condenser
e	evaporator
s	heat source
P	pump
T	turbine
net	net power
th	thermal efficiency
wf	working fluid

REFERENCES

Angelino, G., Paliano, P.C.D., 1998, Multicomponent Working Fluids For Organic Rankine Cycles (ORCs), *Energy*, vol. 23, no. 6: p. 449–463.

Dai, X.Y., Shi, L., Qian, W.Z., 2019, Thermal Stability of Hexamethyldisiloxane (MM) as a Working Fluid for Organic Rankine Cycle. *International Journal of Energy Research*, vol. 43: p. 896-904.

Dong, B.S., Xu, G.Q., Cai, Y.i., et al., 2014, Analysis of zeotropic mixtures used in high-temperature Organic Rankine cycle, *Energy Convers Manage*, vol. 84: p. 253–260.

Erhart, T.G., Gölz, J., Eicker, U., et al., 2016, Working Fluid Stability in Large-Scale Organic Rankine Cycle-Units Using Siloxanes—Long-Term Experiences and Fluid Recycling, *Energies*, vol. 9, no. 6: p. 422.

Keulen, L., Gallarini, S., Landolina, C., et al., 2018, Thermal stability of hexamethyldisiloxane and octamethyltrisiloxane, *Energy*, vol. 165: p. 868-876.

Kim, I.S., Kim, T.S., Lee, J.J., 2017, Off-design performance analysis of organic Rankine cycle using real operation data from a heat source plant. *Energy Convers Manage*, vol. 133: p. 284–291.

Oyekale,J., Heberle, F., Petrollese, M., et al., 2020, Thermo-economic evaluation of actively selected siloxane mixtures in a hybrid solar-biomass organic Rankine cycle power plant, *Applied Thermal Engineering*, vol. 165.

Preißinger, M., Brüggemann, D., 2016, Thermal Stability of Hexamethyldisiloxane (MM) for High-Temperature Organic Rankine Cycle (ORC). *Energies*, vol. 9, no. 3: p. 183.

Rajabloo, T., Bonalumi, D., Iora, P., 2017, Effect of a partial thermal decomposition of the working fluid on the performances of ORC power plants, *Energy*, vol. 133: p. 1013-1026.

Shu, G.Q., Liu, P., Tian, H., et al., 2017, Operational profile based thermal-economic analysis on an Organic Rankine cycle using for harvesting marine engine's exhaust waste heat, *Energy Convers Manage*, vol. 146: p.107–123.

Strzalka, R,. Schneider, D., Eicker, U., 2017, Current status of bioenergy technologies in Germany, *Renew Sustain Energy Rev*, vol. 72: p. 801–820.

Tchanche, B.F., Lambrinos, G., Frangoudakis, A., et al., 2011, Low–grade heat conversion into power using organic Rankine cycles – A review of various applications, *Renew Sustain Energy Rev*, vol. 15, no. 8: p. 3963–3979.

Thomas, Tartière., Marco, Astolfi., 2017, A World Overview of the Organic Rankine Cycle Market, *Energy Procedia*, vol.129: p. 2–9.

Tian, H., Chang, L., Gao, Y., et al., 2017, Yan N. Thermo-economic analysis of zeotropic mixtures based on siloxanes for engine waste heat recovery using a dual-loop organic Rankine cycle (DORC), *Energy Convers Manage*, vol. 136: p. 11–26.

Velez, F., Segovia.,J.J., Martin MC, et al., 2012, A technical, economical and market review of organic Rankine cycles for the conversion of low-grade heat for power generation, *Renew Sustain Energy Rev*, vol. 16, no. 6: p. 4175–4189.

Yildirim, D., Ozgener, L., 2012, Thermodynamics and exergoeconomic analysis of geothermal power plants. *Renew Sustain Energy Rev*, vol. 16, no. 8: p. 6438–6454.

Zhang, T., Liu, L.C., Hao, J.H., et al., 2021, Correlation analysis based multi-parameter optimization of the organic Rankine cycle for medium- and high-temperature waste heat recovery, *Applied Thermal Engineering*, vol. 188.

Zhou, Y., Zhang, F., Yu, L., 2016, Performance analysis of the partial evaporating organic Rankine cycle (PEORC) using zeotropic mixtures. *Energy Convers Manage*, vol. 129: p. 89–99

ACKNOWLEDGEMENT

This work was supported by the National Natural Science Foundation of China (51806117), the National Key Research and Development Plan (2016YFB0901405), and the Science Fund for Creative Research Group (No. 51621062).